TYCHO CRATER RAYS – SMALL CRATERS DISTRIBUTION PATTERNS. R. Bugiolacchi[1,2], [1]Space Science Laboratory, M.U.S.T., Avenida Wai Long, Taipa, Macau - rbugiolacchi@must.edu.mo, [2]Dept. of Earth Sciences, University College London, Gower Street, WC1E 6BT, London, UK – roberto.bugiolacchi@ucl.ac.uk.

Introduction: Smaller craters are not considered statistically significant for Absolute Age Modelling (AMA) principally [1] because of their limited lifetime, which produces a size-dependent steady-state distribution (an 'upper wall'), and the occurrence of secondary craters, which skews the crater density count and are difficult to differentiate from primaries. Thus, few studies have carried out large-scale surveys of sub-hectometer lunar craters. For instance, [2] set the lower limit at 63 m stating that the noted production rollover (a drop-off in density) could be due to crater erasure and not detectability. This work aims at investigating and constrain the size-frequency distribution (SFD) of craters ≤ 30 m in diameter including areas with undisputed secondaries contribution. High-resolution NAC images [3] offer the opportunity of surveying the crater populations of both Tycho's rays and their surrounding regions (Fig. 1).

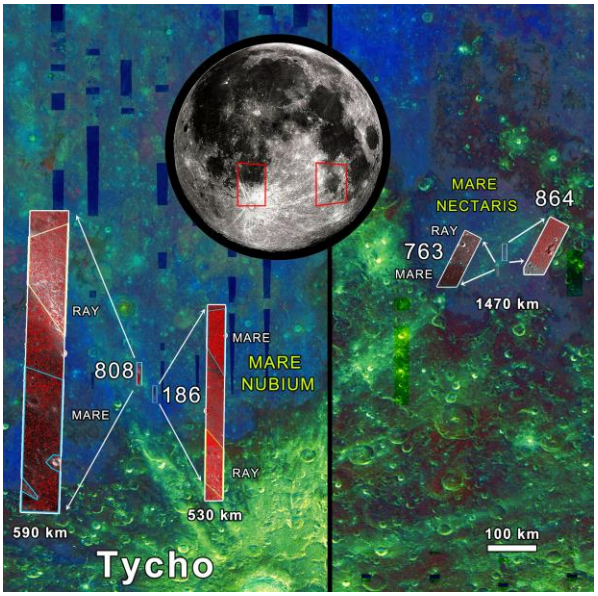

Figure 1. Areas under investigation. NAC images [3] M1180249**808**RE, M111722**186**LE, M183288**763**RE, and M1111570**864**RE, res. ~0.9, 0.5, 0.8, and 1.6 px/m; illumination inc. angle (deg.) ~31, 39, 44, and 74 respectively. Background WAC image [3] and edited Clementine FC mosaic [4]. "km" in figures relate to the average distance from Tycho.

Data and method: Aiming to maintain the highest level of uniformity in the marking environment, each NAC image was layered on one ArcGIS project page (ArcMap 10.2) using the same coordinate system, map projection (Equirectangular Moon) and geographic projection (GCS_MOON). About 100,000 craters ≤ 30 m in diameter were surveyed by the author and marked using 'craterTools' [5]. The lowest size-confidence threshold was set between 4 and 9 meters according to the NAC's pixel resolution. Each area was selected to minimise cross-over terrains (Fig. 2) and named according to the last three digits in the NAC image adding either R (Ray) or M (Mare) suffixes. The SFD data of the resulting ~30,000 craters were plotted using log-log histograms using 1-meter binning (the narrowest possible size range) and shown in Fig. 3.

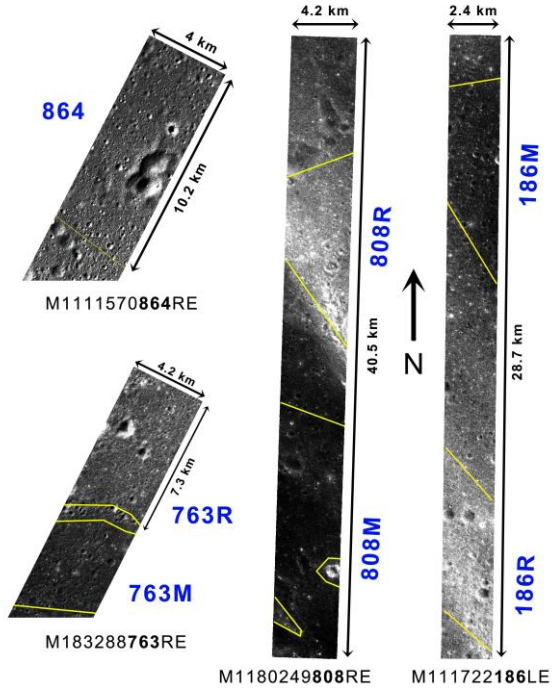

Figure 2. Selected areas of interest and nomenclature.

Results: *Cumulative Histograms*. Three cumulative log-log histograms show craters' SFD data according to the NACs' locations (Fig. 3). The differences in image resolution make a difference on the number/density of surveyed craters: M*186, with the best spatial resolution of 0.5 m/px against ≥0.8 m for the others, hints at a potentially 'straight' power-law cumulative trend for all other regions too (Fig. 3-b). Further, the SFD similarities in the M*186 area suggest that the surface brightness is not correlated to the density of small 'new' craters but it is most likely due to the surge-led surface upturning, which exposed brighter, i.e. less weathered regolith.

NAC*808 instead (Fig. 3-a) shows a clearer difference in density between the upper (R) and lower (M) areas, although they appear to converge around the 30-m diameter. The rollover at ~8 m is consistent with the lower image resolution. The three areas in Mare Nectaris, although representing very different surface morphologies (Fig. 2), share very similar SFDs (Fig. 3-c). Cumulative fits have indexes between -2.6 and -2.4 except for 808M and 186M (-2.0 and -2.1 respectively).

Relative Crater Frequency. In a relative representation of craters, the number of craters within a range, in this case 9-100 m in 1 m bins, is normalized to 100 (%) for ease of comparison (only ≤ 30 m range are plotted here). Fig. 3-d shows a consistent trend among crater size distribution in Mare Nubium, with shared characteristics. The relation between bin sizes are nearly identical for NAC*186, irrespective to location, suggesting a 'ray signature', see for instance 16-20 m. These three units share a power relation with a -3.1 slope. The 'signature' trend is even more evident within Mare Nectaris (Fig. 3-e) with the three units showing similar relative distributions. Also, note that the plotting is in a log-log system so the differences in the larger bin sizes are much exaggerated in comparison to the smaller ones.

AMAs. Last, the crater data were plotted using CraterstatsII [6], and Absolute Modelled Ages derived for completeness. All ages are in the range between 20 Ma (808M) and 40 Ma (763M and rays). Other six areas were included in a comparative study of AMAs (from Mare Tranquillitatis and Mare Serenitatis), not shown here, and they all fall within the same range: 30 ± 10 Ma. One interpretation is that the lower age estimates may represent the Neukum SFD equilibrium fits for the lunar maria (in this range size) and instead the upper values the saturation point.

Conclusions: There is evidence that lunar craters might not display a 'production rollover' but this could be due solely to image resolution limits. Indeed, small craters were mapped down to four meters in diameter and they show a cumulative crater frequency that is consistent with a power law distribution. Surge materials that formed the distinct Tycho's rays produced craters of sizes that have a distinct relative distribution. This is more evident when the crater diameter representation is compared in terms of number of craters per bin, as in the case of Mare Nectaris (crater size range 9-100 m).

It is likely that the crater production equilibrium for mature mare surfaces approaches a cumulative slope of -2 and for the saturated rays of around -2.5, in the size range under investigation.

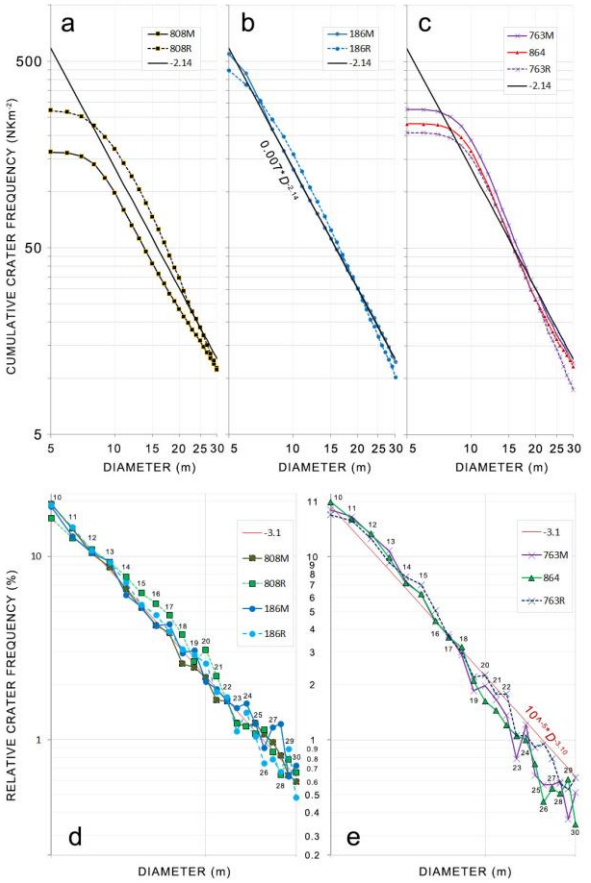

Figure 3. a-c Cumulative craters SFD; d-e Relative crater distribution expressed as percentage: for instance, in 'd' the 11-12 m craters represent around 12% of all craters between the 9-100 m range. Fit lines represent: $M_{cum} = C*D^{\alpha}$, where M is cumulative frequency (Nkm^{-2}), *C* a parameter sensitive to the crater production/destruction of the area, *D* is the crater diameter (km), and α the slope of the curve

Absolute Modelled Ages derived using established methodology [6] cluster around the 30 Ma mark, with the most saturated terrains showing 'ages' close to 40 Ma, with those least affected by secondaries about 20 Ma.

Future work will add several additional areas and will test the hypothesis and conclusions offered in this work.

This study was supported by the Macau Science and Technology Development Fund 039/2013/A2

References: [1] Neukum G. (1977) *Mat. & Phys. Sci., 1327,* 267-272. [2] Dundas C. M. and NcEwen A.S. (2007) *Icarus,* 186, 31-40. [3] Robinson M. S. et al. (2005) *LPS XXXVI,* 1344–1345. [4] Nozette S. et al. (1994) *Science, 266, 1835-1839*. [5] Kneissl T. et al. (2011) *Planet. Space Sci*., 59, 1243-1254. [6] Michael H.J. and Neukum G. (2010) *Earth Planet Sci. Lett*., 294, 223-229.